Post-annealing, fractographic and corrosion failure analyses on tri-modal Mn-particulate Al/Cu multilayered composites

Morteza Alizadeh, Mohammad Samiei, Erfan Salahinejad

This is the accepted manuscript (postprint) of the following article:
M. Alizadeh, M. Samiei, E. Salahinejad, *Post-annealing, fractographic and corrosion failure analyses on tri-modal Mn-particulate Al/Cu multilayered composites*, Vacuum, 139 (2017) 87-92.
https://doi.org/10.1016/j.vacuum.2017.02.017

Post-annealing, fractographic and corrosion failure analyses on tri-modal Mn-particulate Al/Cu multilayered composites

Morteza Alizadeh [a, *], Mohammad Samiei [a], Erfan Salahinejad [b]

[a] *Department of Materials Science and Engineering, Shiraz University of Technology, Modarres Blvd., 71557-13876, Shiraz, Iran*

[b] *Faculty of Materials Science and Engineering, K.N. Toosi University of Technology, Tehran, Iran*

* Corresponding author. E-mail address: Alizadeh@sutech.ac.ir (M. Alizadeh)

Abstract

In this work, Mn-particulate Al/Cu multilayered (70Al/25Cu/5Mn) composites were fabricated by the accumulative roll bonding (ARB) process. Afterwards, the structure (after ARB and post-annealing) and failure (tensile fracture and corrosion in 3.5 wt% NaCl solution) studies were conducted on the specimens processed for different ARB cycles. Based on the results, no intermetallic compound was formed in the ARB-processed composites even to 9 cycles. Nonetheless, Al-Cu-(Mn) intermetallics were detected in the annealed samples, so that their amount was enhanced by increasing ARB cycle. Concerning the failure analyses, the resistance of the produced composites against corrosion and fracture, contrary to strength, was reduced by increasing ARB cycles.

Keywords: Composites; Accumulative roll bonding; Reaction annealing; Failure

This is the accepted manuscript (postprint) of the following article:
M. Alizadeh, M. Samiei, E. Salahinejad, *Post-annealing, fractographic and corrosion failure analyses on tri-modal Mn-particulate Al/Cu multilayered composites*, Vacuum, 139 (2017) 87-92.
https://doi.org/10.1016/j.vacuum.2017.02.017

1. Introduction

Accumulative roll bonding (ARB) as a severe plastic deformation (SPD) method can be used to produce nanostructured and composite sheets. In this regard, a number of bimetal multilayered composites from, for example Al/Ti [1], Al/Cu [2], Zr/Ti [3], Cu/Ag [4], and Al/Zn [5] systems, have been manufactured by ARB and other roll bonding processes. This process has been also used to fabricate various tri-modal multilayered composite of, such as Cu/ Zn/Al [6] and Ti/Al/Nb [7] systems. Depending on the constituents of multi-metal composites, the formation of intermetallic compounds (IMCs) between/among them is likely during ARB and/or post-annealing which is frequently conducted to alter the bond strength [8]. This can affect the performance of the composite, so it should be considered.

Al/Cu composites are under consideration because Cu simultaneously improves the strength, toughness and electrical conductivity of Al [9]. For ARB-processed Al/Cu composites, the formation of Cu_9Al_4, Al_2Cu, and AlCu IMCs after annealing at the interface of the constitutes has been reported [10]. On the other hand, the incorporation of Mn into Al-Cu bimetals can alter some characteristics of the product (especially hardness and strength), developing Al/Cu/Mn composites or alloys which are age-hardenable and ferromagnetic. As a new class of composite materials, for the first time, this work aims at investigating the formation of IMCs during ARB and post-annealing, corrosion behavior and fracture mechanism (as two typical failure sources) of Al/Cu/Mn composites produced ARB.

This is the accepted manuscript (postprint) of the following article:
M. Alizadeh, M. Samiei, E. Salahinejad, *Post-annealing, fractographic and corrosion failure analyses on tri-modal Mn-particulate Al/Cu multilayered composites*, Vacuum, 139 (2017) 87-92.
https://doi.org/10.1016/j.vacuum.2017.02.017

2. Experimental procedures

The starting materials used to fabricate Al/Cu/Mn (70/25/5 in wt %) composites are listed Table 1. To fabricate the composites, first Al strips and Cu foils were annealed, washed in acetone and scratch brushed. Afterwards, three Al strips and two Cu foils were stacked alternatively over each other, where the Mn powder was dispersed between them. The ARB process was carried out on the specimens according to Refs. [11,12]. Afterwards, the composite samples processed to 5 and 9 cycles of ARB, after encapsulation in evacuated quartz tubes, were heat-treated at 300 ºC for 5 h to evaluate the possible formation of intermetallic compounds. Optical microscope (OM) and scanning electron microscope (SEM) were used for the microstructural observation of the produced samples. The phase analysis of the produced samples was also conducted by the X-ray diffraction (XRD) method using Cu Kα1 radiation (λ = 0.15406 nm).

Table 1. Raw materials used in this work

Materials	Form	Length (mm)	Width (mm)	Thickness (mm)	Particle size (μm)
Aluminum 1100	Strip	150	30	0.8	-
Commercially pure copper	Foil	150	30	0.15	-
Manganese	Powder	-	-	-	40

Two typical failure mechanisms (fracture and corrosion) of the processed composites were also studied. Aiming at determining the rupture mode of the as-ARB-processed composite specimens, fracture surfaces after tension to failure were studied by SEM. To support the conclusions drawn from this evaluation, the total elongation of the samples is also reported. Also, to evaluate the corrosion behavior of the produced composite specimens, they were polished mechanically by grit sand papers (up to # 2000) and cleaned in ethanol. Then, the

This is the accepted manuscript (postprint) of the following article:
M. Alizadeh, M. Samiei, E. Salahinejad, *Post-annealing, fractographic and corrosion failure analyses on tri-modal Mn-particulate Al/Cu multilayered composites*, Vacuum, 139 (2017) 87-92.
https://doi.org/10.1016/j.vacuum.2017.02.017

corrosion performance of the produced composites was investigated in a conventional three electrode cell with a platinum plate as the auxiliary electrode and Ag/AgCl as the reference electrode in a 3.5% NaCl solution at 25 ºC, using a potentiostat/galvanostat device (Vertex, Ivium Technologies). The corrosion current density (i_{corr}) and corrosion potential (E_{corr}) of the produced composites were determined from the intersection of the anodic and cathodic Tafel curves using the Tafel extrapolation method.

3. Results and discussion

Fig. 1 shows the XRD pattern of the Al and Cu constitutes prior to the ARB process, as well as that of the Al/Cu/Mn composite after 9 cycles of ARB. As can be seen, the composite only consists of the initial materials (i.e. Al, Cu, and Mn) after nine cycles, so that no intermetallic phases were detected by this analysis. This suggests that the ARB process can not cause to reactions between/among the Al, Cu, and Mn constitutes, due to the slow interdiffusion of the constitutive atoms during ARB. In agreement with this work, no intermetallic phases were detected in ARB-processed Al/Cu composites prior to annealing [10]. It means that the addition of Mn does not result in the formation of IMCs during ARB. In contrast, the $CuZn_5$ intermetallic is formed during ARB of Cu/Zn/Al multilayers [13].

This is the accepted manuscript (postprint) of the following article:
M. Alizadeh, M. Samiei, E. Salahinejad, *Post-annealing, fractographic and corrosion failure analyses on tri-modal Mn-particulate Al/Cu multilayered composites*, Vacuum, 139 (2017) 87-92.
https://doi.org/10.1016/j.vacuum.2017.02.017

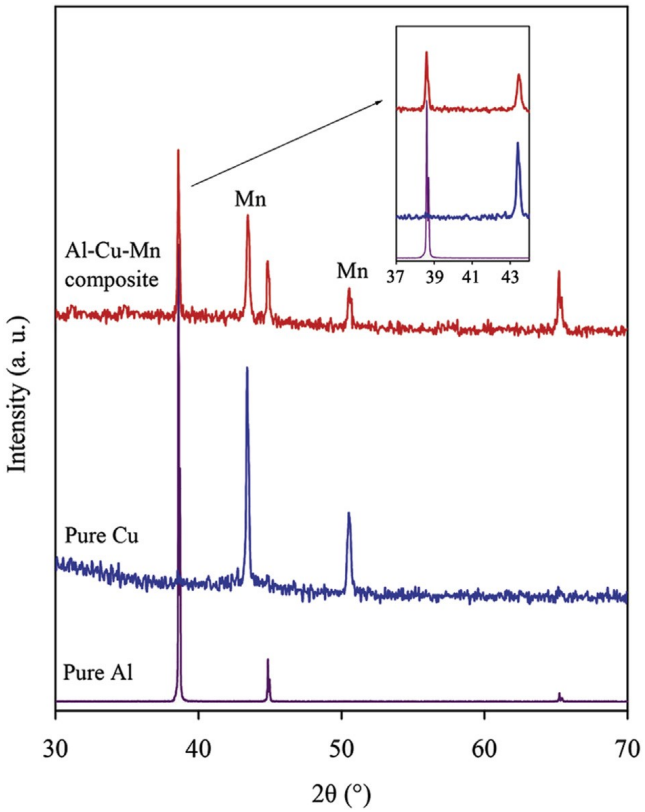

Fig. 1. XRD pattern of the as-received Al (a), as-received Cu (b) and Cu/Al/Mn composite produced by nine cycles of ARB (c).

By comparing the XRD patterns of the pure elements and the composite, the peak broadening of the composite is evident, which is attributed to the effects of strain and structural refinement in the produced composites. The crystallite sizes of the samples were calculated using the Rietveld XRD method. According to the quantitative XRD results, the crystallite size of Al and Cu reached 190 and 85 nm, respectively, after 9 ARB cycles. The structure refinement during the ARB process can be explained by the increase in strain, the formation of interfaces between layers [14], and subdivision from low-angle to high-angle boundaries [15-22]. Moreover, the smaller crystallite size of Cu than Al at the ARB process is attributed

This is the accepted manuscript (postprint) of the following article:
M. Alizadeh, M. Samiei, E. Salahinejad, *Post-annealing, fractographic and corrosion failure analyses on tri-modal Mn-particulate Al/Cu multilayered composites*, Vacuum, 139 (2017) 87-92.
https://doi.org/10.1016/j.vacuum.2017.02.017

to the lower stacking fault energy of Cu (78 mJ/m^2) than Al (166 mJ/m^2) [23]. In the copper layers, the recombination and cross-slipping of dislocations during the ARB process are difficult to occur due to its low stacking fault energy. Therefore, the crystallite size can be decreased and reached about 85 nm. While in the aluminum layers, with a high stacking fault energy, the crystallite size cannot be decreased like copper and reached about 190 nm, due to continuous dynamic recovery and recrystallization.

The microstructure of the ARB-processed composites after second and ninth ARB cycles was also characterized by SEM, as shown in Fig. 2. In accordance with Fig. 2a and b, continuous Cu layers of about 55 μm in thickness with no crack and delamination are observed in the composite processed for second ARB cycles. By progression of ARB to nine cycles, the thicknesses of both the layers were not only decreased, but also the Cu layers were necked and ruptured due to its high work hardening, while the Al layers kept its continuity. In fact, the difference between the stacking fault energies of Cu and Al leads to the greater work hardening rate of Cu than Al. Consequently, in the final ARB cycles (Fig. 2c), a composite of the continuous Al matrix with homogeneously-distributed Cu fragments with a wide range of about 5-30 μm in thickness was achieved. In agreement with the XRD analysis, no new phases were observed in the SEM images.

This is the accepted manuscript (postprint) of the following article:
M. Alizadeh, M. Samiei, E. Salahinejad, *Post-annealing, fractographic and corrosion failure analyses on tri-modal Mn-particulate Al/Cu multilayered composites*, Vacuum, 139 (2017) 87-92.
https://doi.org/10.1016/j.vacuum.2017.02.017

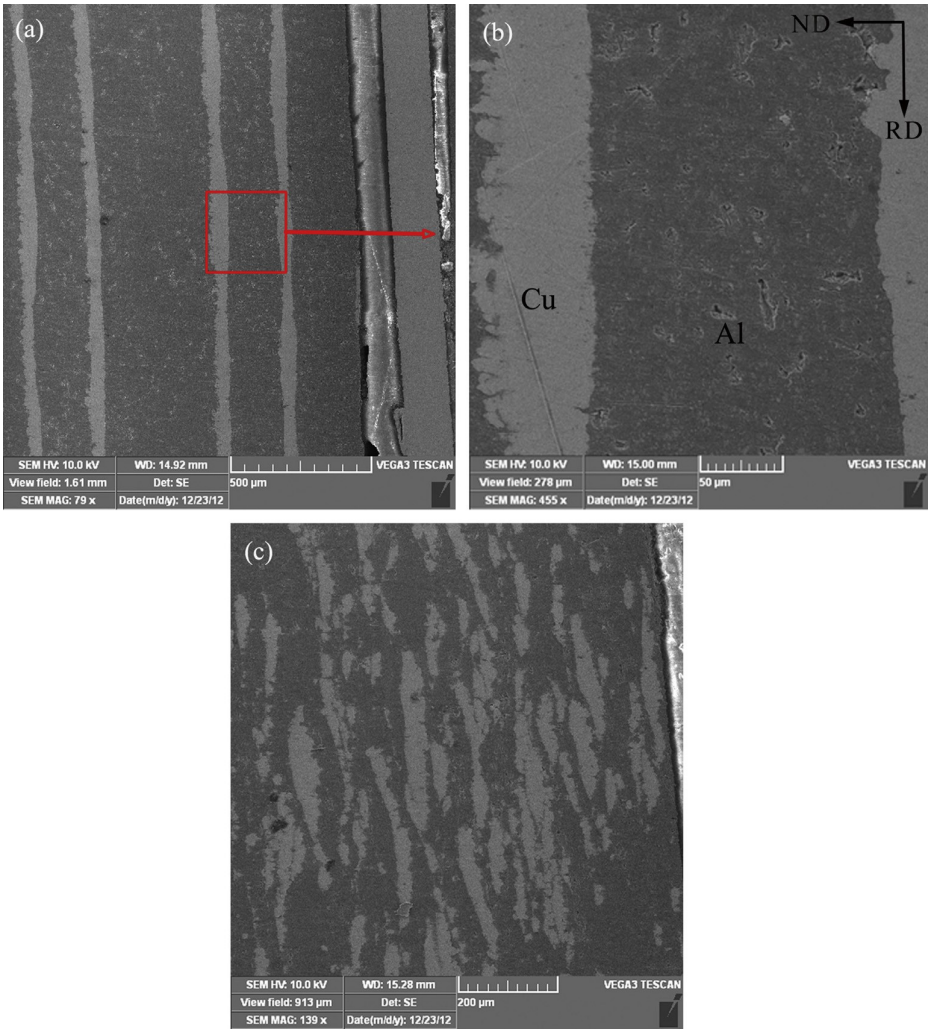

Fig. 2. SEM micrographs of the composites produced by two (a and b) and nine (c) cycles of ARB.

Fig. 3 indicates the OM image of the composite produced by 9 ARB cycles after annealing. The formation of new phases due to annealing is obvious, so that the red, dark, and light regions represent Cu, Al, and intermetallics, respectively. In order to confirm the formation of intermetallics, the XRD analysis was conducted on the heat-treated composites. Fig. 4 shows the XRD patterns of the composite produced by 5 and 9 cycles of ARB after heat treatment.

This is the accepted manuscript (postprint) of the following article:
M. Alizadeh, M. Samiei, E. Salahinejad, *Post-annealing, fractographic and corrosion failure analyses on tri-modal Mn-particulate Al/Cu multilayered composites*, Vacuum, 139 (2017) 87-92.
https://doi.org/10.1016/j.vacuum.2017.02.017

As can be seen, three intermetallic phases were formed in the both samples, suggesting the occurrence of reactions among Al, Cu, and Mn. Indeed, the heat energy of the annealing process accelerated the interdiffusion of the constitutes to form the intermetallic compounds. The quantitative results of the XRD test are listed in Table 2. By comparing the XRD patterns of the composite before and after heat treatment (Figs. 1 and 4), it is revealed that the intensity of the initial elements was decreased, which is because of the consumption of the base metals (i.e. Al and Cu) as a result of the intermetallic formation. Furthermore, by increasing ARB cycles, an increase in the amount of the intermetallics after the same annealing process is obtained, owing to the more homogeneously distributed Cu fragments and the reduction of the diffusion paths. However, the formation of AlCu, Al_2Cu and Al_4Cu_9 IMCs has been reported in Al/Cu multilayers after 8 cycles of ARB and annealing at 300 ºC [10]. It suggests that in the tri-metal composites, Mn inhibits the formation of AlCu; in return, $AlCu_2Mn$ is formed.

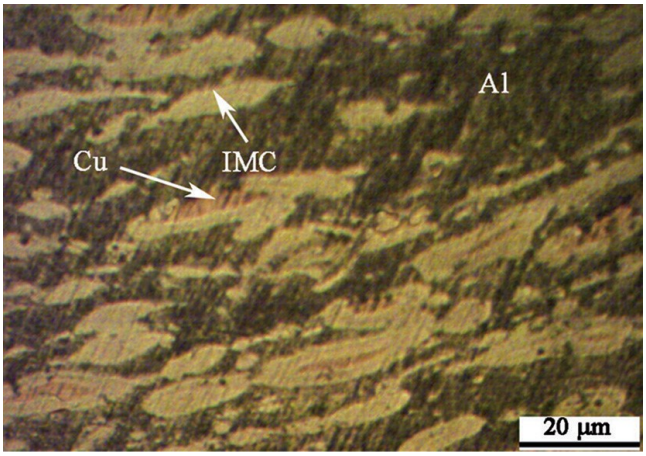

Fig. 3. Optical micrograph of the composite produced by 9 cycles of ARB after annealing at 300 ºC.

This is the accepted manuscript (postprint) of the following article:
M. Alizadeh, M. Samiei, E. Salahinejad, *Post-annealing, fractographic and corrosion failure analyses on tri-modal Mn-particulate Al/Cu multilayered composites*, Vacuum, 139 (2017) 87-92.
https://doi.org/10.1016/j.vacuum.2017.02.017

Table 2. Quantitative values of the phases existing in the composites produced for 5 and 9 ARB cycles after annealing.

Phase	wt%	
	5 Cycle	9 Cycle
Al	56	30
Cu	4	3
Al_2Cu	30	50
Al_4Cu_9	6	11
$AlCu_2Mn$	4	6

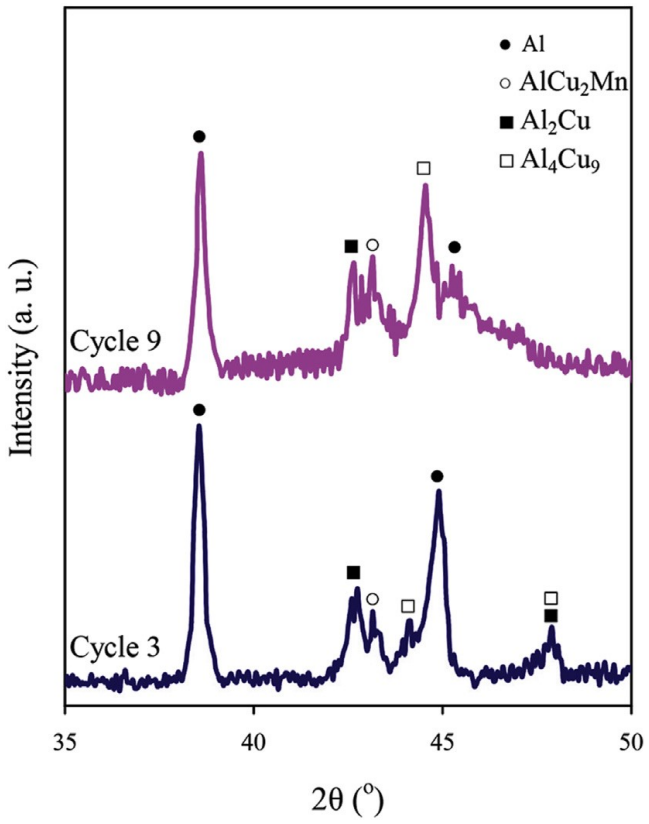

Fig. 4. XRD pattern of the Cu/Al/Mn composite processed by various ARB cycles after annealing at 300 ºC.

This is the accepted manuscript (postprint) of the following article:
M. Alizadeh, M. Samiei, E. Salahinejad, *Post-annealing, fractographic and corrosion failure analyses on tri-modal Mn-particulate Al/Cu multilayered composites*, Vacuum, 139 (2017) 87-92.
https://doi.org/10.1016/j.vacuum.2017.02.017

According to the Al-Cu phase diagram [24], among five equilibrium intermetallic phases (AlCu, Al_2Cu Al_2Cu_3, Al_3Cu_4, and Al_4Cu_9), only Al_4Cu_9 and Al_2Cu were detected in this study in Cu-rich and Al-rich areas, respectively. Moreover, since the solubility limit of Cu in Al (2.48 at%) is less than that of Al in Cu (19.7 at%) [25], the Al-Cu solid solution would be expected to saturate first, resulting in the nucleation of Al_2Cu at the bonded interface. Furthermore, since the diffusion rate of Cu in Al ($D_{Cu/}$ Al = 6.5×10^5 m^2 s^{-1}) is higher than that of Al in Cu ($D_{Al/}$ Cu = 4.5×10^6 m^2 s^{-1}) [10,26], Cu atoms can diffuse into the Al side rapidly and form Al_2Cu at the initial stage. The nucleation of qAl_2Cu at the Al-Cu interface as the first compound has been previously reported [10,27,28]. Afterwards, the more diffusion of Cu and Al into each other as well as Cu atoms into Al_2Cu resulted in the production of Al_4Cu_9 via a diffusion reaction (Al_2Cu þ Cu/Al_4Cu_9). It was shown that at low Al concentrations (Cu-rich areas), Cu and Al react at low temperatures and form g-Cu_9Al_4, while g-Cu_9Al_4 is dissolved into Cu at high temperatures [29]. From the thermodynamic point of view, since the absolute value of the effective free energy of Al_2Cu is the largest among all of the possible intermetallics, it is most likely to emerge as the first phase. In addition to the effective free energy, the formation energy can estimate the first phase production. According to the literature [27], the formation energies of Al2Cu and Al4Cu9 are 0.78 eV and 0.83 eV, respectively. Subsequently, the formation energy calculation suggests that the Al4Cu9 has the tendency to nucleate after Al2Cu at the interface [28].

The effect of the number of ARB cycles on the microstructure of the heat-treated Al/Cu/Mn composites is shown in Fig. 5. As it can be seen from Fig. 5a, continuous new intermetallic layers were formed at the interface of the sample processed by 5 ARB cycles. By decreasing the layers thickness for the composite fabricated by nine cycles of ARB (Fig. 5b), a thicker intermetallic layer is well recognizable. Note that by the reduction in the Al and Cu layer

This is the accepted manuscript (postprint) of the following article:
M. Alizadeh, M. Samiei, E. Salahinejad, *Post-annealing, fractographic and corrosion failure analyses on tri-modal Mn-particulate Al/Cu multilayered composites*, Vacuum, 139 (2017) 87-92.
https://doi.org/10.1016/j.vacuum.2017.02.017

thickness, grain refinement as well as the increase in the total area of the interfaces occur during the ARB process, leading to increase in the number of nucleation sites. Hence, the amount of the intermetallic phases was increased by progression of the ARB process up to nine cycles. The increase in the intermetallic layer thickness by progression of ARB can be also realized from the XRD analysis (Table 2), as it causes the increase in the quantity of the intermetallics.

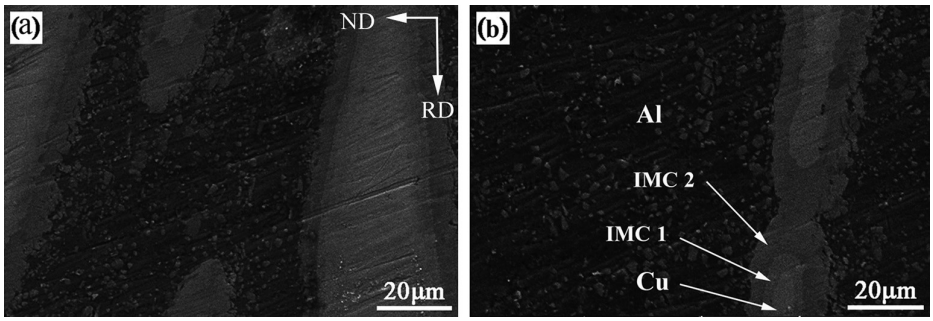

Fig. 5. SEM micrographs of the composites processed by two (a) and nine (b) ARB cycles after annealing at 300 ºC, where IMC1 and IMC2 are Al_4Cu_9 and Al_2Cu, respectively.

In order to recognize the rupture mechanism of the produced composites, the tensile fracture surfaces of the Al/Cu/Mn composites processed for 2, 5 and 9 cycles of ARB (without subsequent annealing) were examined by SEM, as shown in Fig. 6. It can be seen that the Al/Cu interface in the Al/Cu/Mn composite is clear after second cycles. With increasing ARB cycles, the bonding quality of the Al/Cu interface is gradually improved. It can be also seen that an appropriate bonding occurs between the former layers for the last ARB cycle (Fig. 6c), due to the increase in rolling pressure and interlayer atom diffusion. This is in agreement with Ref. [30] in which by increasing the thickness reduction, the weld efficiency of two stacked

strips was increased. Accordingly, by increasing the weld efficiency, the bonding quality of the Al/Cu interface is improved.

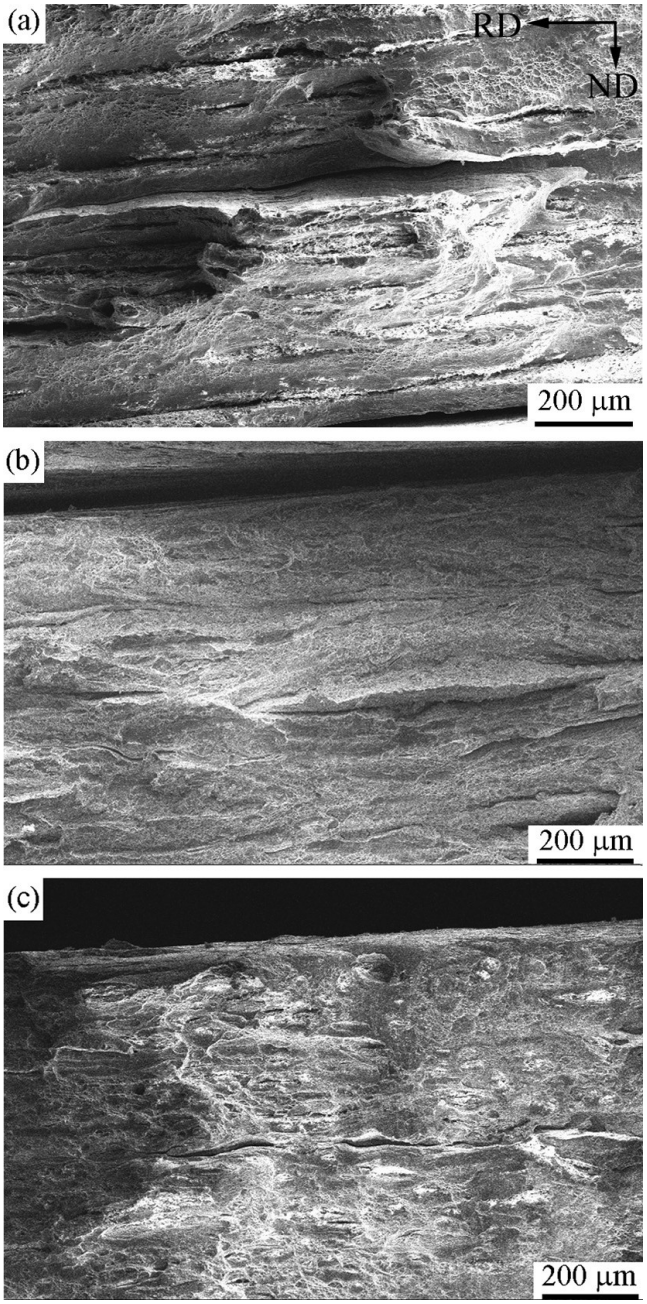

Fig. 6. Fracture surfaces of the Al/Cu/Mn composites after 2 (a), 5 (b), and 9 (c) cycles.

The fracture appearance of the composite after 2 cycles of ARB in a higher magnification (Fig. 7a) reveals that there are areas with shallow shear dimples and also areas with an almost

flat feature. This indicates that the fracture mode in the initial cycles is a mixture of ductile and brittle. The portion of ductile fracture occurs by the formation and coalescence of microvoids, whereas the shallow shear dimples are produced by a simple shear deformation [2]. The areas including dimples are decreased by increasing the rolling cycles, while the flat areas, indicative of brittle surfaces, are increased. The fracture surface of the sample after 9 cycles of ARB in a higher magnification (Fig. 7b) specifies that the brittle fracture is dominated because the flat area has been increased. On the other hand, it has been reported that the dominant fracture mechanism of bimetal Al/Cu multilayers is shear ductile fracture [2]. On comparison, it is speculated that the incorporation of Mn gives rise to the increase of brittleness. Also, the increase of brittleness with ARB cycles is verified by the decrease observed in the total elongation extracted from the tensile tests (Fig. 8).

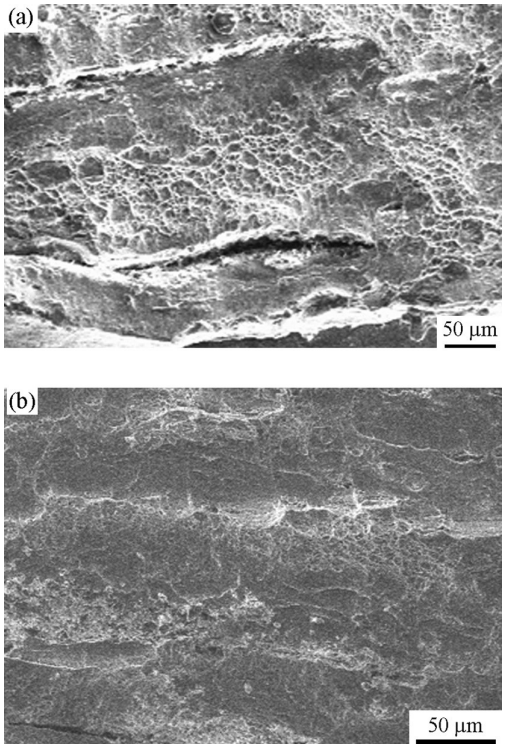

Fig. 7. Fracture surface of the Al/Cu/Mn composites after 2 (a) and 9 (b) cycles at higher magnifications than Fig. 6.

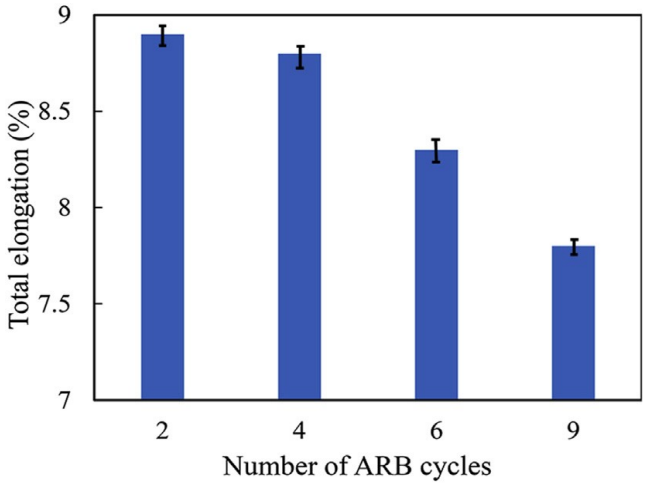

Fig. 8. Total elongation of the ARB-processed composite samples.

The potentiodynamic polarization curves of the as-ARBed composite samples in the 3.5% NaCl solution and extracted electrochemical parameters are shown in Fig. 9 and Table 3, respectively. As it can be seen, the corrosion potential of the composite calculated by the Tafel extrapolation is negative and becomes more negative by progression of the ARB process. Also, the corrosion current density (i_{corr}) is increased by increasing the number of ARB cycles, indicating lower corrosion resistance. Indeed, by increasing the ARB cycles, the enhancement in the level of interfaces (based on Fig. 2), dislocation density and strain [31] deteriorates the corrosion resistance. Also, in the produced Al/Cu/Mn composites, the presence of an active element (i.e. Mn) [32] leads to a decrease in the corrosion potential, compared to pure Al and Al/Cu multilayers [33]. It is known that aluminum and its alloys are reactive materials and have a tendency to corrosion and oxidation with atmospheric oxygen, forming a surface film. The corrosion resistance and passive behavior of the formed oxide layer of the alloy are strongly affected by the chemical composition of the alloy and electrolyte properties (such as temperature, Cl content, and pH). However, aggressive anions, like Cl, lead to film breakdown and increase the corrosion rate. The corrosion mechanism of aluminum and its alloys in neutral solutions is based on aluminum dissolution from the flawed

regions or active sites of the formed barrier film. At the presence of Cl ions in the solution, some reactions, including the formation of $AlCl_2$ and $AlCl_3$ take place [34]. Therefore, the chloride ions penetrate into the surface film and react with the flawed regions, forming corrosion products. The predominant mechanism is the adsorption of chloride ions upon the anodic areas (i.e. Bared metal or flawed regions), which prevents the repair process [35]. In the case of the Al/Cu/Mn composites, the presence of Mn and Cu on the surface increases the number of flawed regions, leading to the formation of active galvanic couples, consequently increases the corrosion rate.

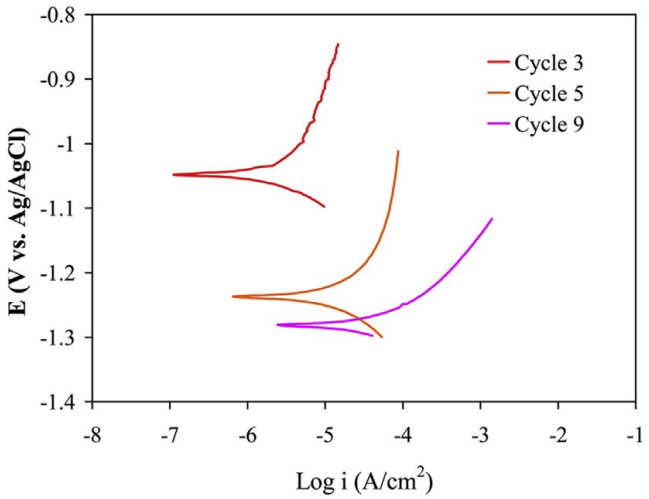

Fig. 9. Potentiodynamic polarization curves of the Al/Cu/Mn composites in the 3.5 wt % NaCl solution.

Table 3. Parameters derived from the potentiodynamic polarization curves for the produced composites at various cycles.

ARB Cycles	E_{corr} (mV vs. Ag/AgCl)	i_{corr} (μA/cm^2)
3	−1.05	1.1
5	−1.24	21.0
9	−1.28	22.3

4. Conclusions

Mn-particulate Al/Cu multilayered composites were produced by the ARB process and some of their properties were investigated. Then, the produced composites samples were annealed at 300 ºC for 5 h and the subsequent structures were investigated. The outcome of this study can be summarized as follows:

1. The XRD analysis showed that no new phases were formed in the ARBed composites even for 9 cycles. Also, the addition of Mn could not lead to the formation of IMCs during ARB.

2. Al_2Cu, Al_4Cu_9 and, $AlCu_2Mn$ intermetallic compounds were detected in the annealed composites, while Mn inhibited the formation of the AlCu intermetallic in the tri-metal composites.

3. By increasing ARB cycles, the areas consisting of dimples were decreased, while the flat areas of the brittle fracture were dominated.

4. By increasing the ARB cycles, the corrosion rate of the produced composites was increased.

Acknowledgements

The authors would like to thank the Shiraz University of Technology (Department of Materials Science and Engineering) due to the support of this study. Also, Mr. Jesmani is acknowledged for his nice help.

References

[1] D. Yang, P. Cizek, P. Hodgson, Wen Ce, Ultrafine equiaxed-grain Ti/Al composite produced by accumulative roll bonding, Scr. Mater. 62 (2010) 321-324.

[2] M. Eizadjou, A.K. Talachi, H.D. Manesh, H.S. Shahabi, K. Janghorban, Investigation of structure and mechanical properties of multi-layered Al/Cu composite produced by accumulative roll bonding (ARB) process, Compos. Sci. Technol. 68 (2008) 2003-2009.

[3] P. Hsieh, Y. Lo, C. Wang, J. Huang, S. Ju, Cyclic transformation between nanocrystalline and amorphous phases in Zr based intermetallic alloys during ARB, Intermetallics 15 (2007) 644-651.

[4] L. Ghalandari, M. Moshksar, High-strength and high-conductive Cu/Ag multilayer produced by ARB, J. Alloys Compd. 506 (2010) 172-178.

[5] R.N. Dehsorkhi, F. Qods, M. Tajally, Investigation on microstructure and mechanical properties of Al-Zn composite during accumulative roll bonding (ARB) process, Mater. Sci. Eng. A 530 (2011) 63-72.

[6] M. Mahdavian, L. Ghalandari, M. Reihanian, Accumulative roll bonding of multilayered Cu/Zn/Al: an evaluation of microstructure and mechanical properties, Mater. Sci. Eng. A 579 (2013) 99-107.

[7] R. Zhang, V.L. Acoff, Processing sheet materials by accumulative roll bonding and reaction annealing from Ti/Al/Nb elemental foils, Mater. Sci. Eng. A 463 (2007) 67-73.

[8] M. Alizadeh, Effects of temperature and B_4C content on the bonding properties of roll-bonded aluminum strips, J. Mater. Sci. 47 (2012) 4689-4695.

[9] M. Alizadeh, M. Talebian, Fabrication of Al/Cu_p composite by accumulative roll bonding process and investigation of mechanical properties, Mater. Sci. Eng. A 558 (2012) 331-337.

[10] C.-C. Hsieh, M.-S. Shi, W. Wu, Growth of intermetallic phases in Al/Cu composites at various annealing temperatures during the ARB process, Metals Mater. Int. 18 (2012) 1-6.

[11] M. Alizadeh, M. Samiei, Fabrication of nanostructured Al/Cu/Mn metallic multilayer composites by accumulative roll bonding process and investigation of their mechanical properties, Mater. Des. 56 (2014) 680-684.

[12] M. Alizadeh, Strength prediction of the ARBed Al/Al_2O_3/B_4C nanocomposites using Orowan model, Mater. Res. Bull. 59 (2014) 290-294.

[13] M. Reihanian, M. Mahdavian, L. Ghalandari, A. Obeidavi, Formation of a solid solution through accumulative roll bonding (ARB) and post-heat treatment of multilayered Cu/Zn/Al, Iran. J. Mater. Form. 1 (2014) 24-31.

[14] M. Chen, H. Hsieh, W. Wu, The evolution of microstructures and mechanical properties during accumulative roll bonding of Al/Mg composite, J. alloys Compd. 416 (2006) 169-172.

[15] S. Lee, Y. Saito, T. Sakai, H. Utsunomiya, Microstructures and mechanical properties of 6061 aluminum alloy processed by accumulative roll-bonding, Mater. Sci. Eng. A 325 (2002) 228-235.

[16] M. Alizadeh, M. Paydar, F.S. Jazi, Structural evaluation and mechanical properties of nanostructured Al/B 4 C composite fabricated by ARB process, Compos. Part B Eng. 44 (2013) 339-343.

[17] S. Mansourzadeh, M. Hosseini, E. Salahinejad, A. Yaghtin, Cu-$(B_4C)_p$ metal matrix composites processed by accumulative roll-bonding, Prog. Nat. Sci. Mater. Int. 26 (2016) 613e620.

[18] M. Alizadeh, E. Salahinejad, A comparative study on metal-matrix composites fabricated by conventional and cross accumulative roll-bonding processes, J. Alloys Compd. 620 (2015) 180-184.

[19] M. Alizadeh, E. Salahinejad, Processing of ultrafine-grained aluminum by cross accumulative roll-bonding, Mater. Sci. Eng. A 595 (2014) 131-134.

[20] A.H. Yaghtin, E. Salahinejad, A. Khosravifard, Processing of nanostructured metallic matrix composites by a modified accumulative roll bonding method with structural and mechanical considerations, Int. J. Miner. Metall. Mater. 19 (2012) 951-956.

[21] A. Yazdani, E. Salahinejad, Evolution of reinforcement distribution in Al-B_4C composites during accumulative roll bonding, Mater. Des. 32 (2011) 3137-3142.

[22] A. Yazdani, E. Salahinejad, J. Moradgholi, M. Hosseini, A new consideration on reinforcement distribution in the different planes of nanostructured metal matrix composite sheets prepared by accumulative roll bonding (ARB), J. Alloys Compd. 509 (2011) 9562-9564.

[23] V.Y. Mehr, M.R. Toroghinejad, A. Rezaeian, Mechanical properties and microstructure evolutions of multilayered Al-Cu composites produced by accumulative roll bonding process and subsequent annealing, Mater. Sci. Eng. A 601 (2014) 40-47.

[24] C. Xia, Y. Li, U. Puchkov, S. Gerasimov, J. Wang, Microstructure and phase constitution near the interface of Cu/Al vacuum brazing using Al-Si filler metal, Vacuum 82 (2008) 799-804.

[25] Y. Guo, G. Liu, H. Jin, Z. Shi, G. Qiao, Intermetallic phase formation in diffusion bonded Cu/Al laminates, J. Mater. Sci. 46 (2011) 2467-2473.

[26] T. Akatsu, N. Hosoda, T. Suga, M. Rühle, Atomic structure of Al/Al interface formed by surface activated bonding, J. Mater. Sci. 34 (1999) 4133-4139.

[27] H. Xu, C. Liu, V. Silberschmidt, S. Pramana, T. White, Z. Chen, A re-examination of the mechanism of thermosonic copper ball bonding on aluminium metallization pads, Scr. Mater. 61 (2009) 165-168.

[28] J. Chen, Y.-S. Lai, Y.-W. Wang, C.R. Kao, Investigation of growth behavior of Al-Cu intermetallic compounds in Cu wire bonding, Microelectron. Reliab. 51 (2011) 125-129.

[29] D. Ying, D. Zhang, Solid-state reactions between Cu and Al during mechanical alloying and heat treatment, J. Alloys Compd. 311 (2000) 275-282.

[30] M. Alizadeh, M. Paydar, Study on the effect of presence of TiH_2 particles on the roll bonding behavior of aluminum alloy strips, Mater. Des. 30 (2009) 82-86.

[31] E. Akiyama, Z. Zhang, Y. Watanabe, K. Tsuzaki, Effects of severe plastic deformation on the corrosion behavior of aluminum alloys, J. Solid State Electrochem. 13 (2009) 277-282.

[32] E. Salahinejad, M. Ghaffari, D. Vashaee, L. Tayebi, Is cell viability always directly related to corrosion resistance of stainless steels? Mater. Sci. Eng. C 62 (2016) 439-443.

[33] M. Abdolahi Sereshki, B. Azad, E. Borhani, Corrosion behavior of Al-2wt% Cu alloy processed by accumulative roll bonding (ARB) process, J. Ultrafine Grained Nanostruct. Mater. 49 (2016) 22-28.

[34] W. Badawy, F. Al-Kharafi, A. El-Azab, Electrochemical behaviour and corrosion inhibition of Al, Al-6061 and Al-Cu in neutral aqueous solutions, Corros. Sci. 41 (1999) 709-727.

[35] A. Mazhar, W. Badawy, M. Abou-Romia, Impedance studies of corrosion resistance of aluminium in chloride media, Surf. Coat. Technol. 29 (1986) 335-345.